Early prediction of neoadjuvant chemotherapy efficacy among patients with triple-negative breast cancer using an ultrasound-based radiomics nomogram

Min-Jia Lin[1]
Hai-Ling Zha[2]
Man-Qi Zhang[3]
Yu Du[4]
Min Zong[5]
Cui-Ying Li[2]

[1]Taizhou Hospital of Zhejiang Province Affiliated to Wenzhou Medical University, Department of Ultrasound, Taizhou, China

[2]The First Affiliated Hospital of Nanjing Medical University, Department of Ultrasound, Nanjing, China

[3]Affiliated Drum Tower Hospital of Nanjing University Medical School, Department of Ultrasound Medicine, Nanjing, China

[4]Shanghai General Hospital, Shanghai Jiao Tong University School of Medicine, Department of Ultrasound, Shanghai, China

[5]The First Affiliated Hospital of Nanjing Medical University, Department of Radiology, Nanjing, China

PURPOSE

To develop and validate a radiomics nomogram based on early ultrasound (US) imaging for predicting pathologic complete response (pCR) in patients with triple-negative breast cancer (TNBC) receiving neoadjuvant chemotherapy (NAC).

METHODS

This retrospective study included 328 patients with TNBC treated between September 2019 and January 2024, divided into a training cohort (n = 230) and a validation cohort (n = 98). Clinicopathologic data, US features before NAC, tumor volume reduction (TVR) after two cycles of NAC, and radiomics features were collected. Multiple logistic regression was applied to identify the potential predictors of pCR. The efficacy of the nomogram was evaluated through the receiver operating characteristic, calibration, and decision curve analyses. The study was approved by the ethics committee on February 28, 2024, with approval number 2023-SR-799, and the requirement for informed consent was waived.

RESULTS

Twelve features were selected to construct the radiomics signature (RS). The nomogram, incorporating tumor histologic grade, TVR, and RS, yielded an area under the curve of 0.856 [95% confidence interval (CI), 0.807–0.905] in the training cohort and 0.836 (95% CI, 0.749–0.923) in the validation cohort, outperforming both the clinico-ultrasonic and RS models. The calibration and decision curves confirmed the nomogram's excellent calibration and clinical utility.

CONCLUSION

The nomogram, which includes US characteristics, clinical variables, and radiomics features, exhibited satisfactory performance in predicting NAC efficacy in patients with TNBC.

CLINICAL SIGNIFICANCE

The US-based radiomics nomogram, incorporating histologic grade, TVR, and RS, shows preliminary clinical application potential for predicting NAC efficacy in patients with TNBC.

KEYWORDS

Triple-negative breast cancer, neoadjuvant chemotherapy, pathologic complete response, radiomics, ultrasonography

Corresponding author: Min Zong, Cui-Ying Li

E-mail: mzong@njmu.edu.cn, lcy_njmu@163.com

Breast cancer has become the most prevalent malignancy in women worldwide and the leading cause of cancer-related mortality, according to the latest global cancer statistics from 2022.[1] Triple-negative breast cancer (TNBC), which is characterized by the absence of estrogen receptor, progesterone receptor, and human epidermal growth factor receptor 2 (HER-2), is more likely to involve lymph nodes and has an early tendency toward recurrence.[2,3] Its heterogeneity and lack of specific molecular targets contribute to its higher likelihood of

early recurrence and poorer prognosis compared with other breast cancer subtypes.[4-7]

Neoadjuvant chemotherapy (NAC) has shown promising results for patients with TNBC by decreasing the tumor burden, increasing the breast-conserving rate, de-escalating axillary surgery, and allowing treatment reorientation in patients with tumor progression.[8] Pathologic complete response (pCR) after NAC has become a surrogate marker for both disease-free survival and long-term overall survival.[9,10] However, histological analysis of surgical specimens, the gold standard for response evaluation, is only accessible following the completion of NAC treatment.[11] Thus, evaluating the response to chemotherapy early in the treatment course to more accurately forecast the likelihood of achieving pCR in patients with TNBC could help clinicians modify ineffective treatments or avoid unnecessary treatment escalation.[12] Imaging methods for predicting the response to NAC include ultrasound (US), magnetic resonance imaging (MRI), and positron emission tomography (PET).[13,14] Compared with MRI and PET, US is more cost-effective and suitable for repeated evaluation during NAC, playing a pivotal role in detecting treatment response.[15] Nevertheless, few studies have examined the correlation between pCR in TNBC and US features, highlighting the need for further investigation into US as an early predictor of NAC response.

Radiomics is a new field of computer-aided technology that extracts and analyzes a large number of quantitative medical image features that are difficult for the human eye to detect, applying these features for clinical decision-making to enhance diagnostic accuracy.[16,17] Previous studies have shown that radiomics can be used to detect disease status, evaluate the response to NAC, and provide valuable information on cancer aggressiveness.[18-20] For the assessment and prediction of early NAC response, radiomics nomograms based on MRI are most widely used, with limited studies utilizing US for therapeutic evaluation.[21] We hypothesized that an early radiomics nomogram combining US features, clinical findings, and a radiomics signature (RS) could provide additional information to estimate the pCR in patients with TNBC.

Therefore, this study aimed to develop an early US-based radiomics nomogram to predict pCR after NAC in patients with TNBC.

Methods

Patients in this study

The retrospective study was approved by the Ethics Committee of The First Affiliated Hospital of Nanjing Medical University, and the requirement for informed consent was waived. The approval number was 2023-SR-799 and approval date was 28 February 2024. A total of 412 consecutive patients with pathologically confirmed TNBC who underwent NAC at our institution between September 2019 and January 2024 were considered, and 84 were excluded. All patients received eight cycles of NAC (taxane- and anthracycline-based chemotherapy regimens) followed by surgery. The inclusion criteria were (i) biopsy-confirmed TNBC without distant metastasis, (ii) US examination performed prior to NAC, (iii) US examination performed after two cycles of NAC, (iv) availability of complete clinicopathologic and US data, and (v) surgery performed after completion of NAC. The exclusion criteria were (i) a history of other tumors, (ii) incomplete NAC or surgery performed at an external institution, (iii) lack of pre-NAC or post-two-cycle NAC US data, (iv) poor-quality US images, and (v) presence of multiple or non-mass lesions. Ultimately, 328 eligible patients (age range: 20–82 years; mean age: 49.4 years) were included and randomly assigned to training and validation cohorts at a ratio of 7:3. The training cohort consisted of 230 patients (pCR: 82, non-pCR: 148), and the validation cohort consisted of 98 patients (pCR: 32, non-pCR: 66). The study flowchart is presented in Figure 1.

Ultrasound imaging acquisition and analysis

All breast US examinations were performed at two time points: before NAC and after two cycles of NAC, using either MyLab Twice (Esaote S.P.A., Italy) or Samsung RS80A (Samsung Medison Co. Ltd., Seoul, South Korea) equipment. The US features collected included the three largest tumor dimensions (length, width, and height) in transverse and

Main points

· A clinico-ultrasonic model combining histologic grade and tumor volume reduction after two cycles of neoadjuvant chemotherapy (NAC) is associated with treatment efficacy in patients with triple-negative breast cancer (TNBC).

· A radiomics signature derived from ultrasound (US) features shows excellent potential for predicting pathologic complete response in patients with TNBC.

· An early US-based radiomics nomogram demonstrates favorable performance in predicting NAC efficacy and may assist clinicians in identifying potential poor pathological responders.
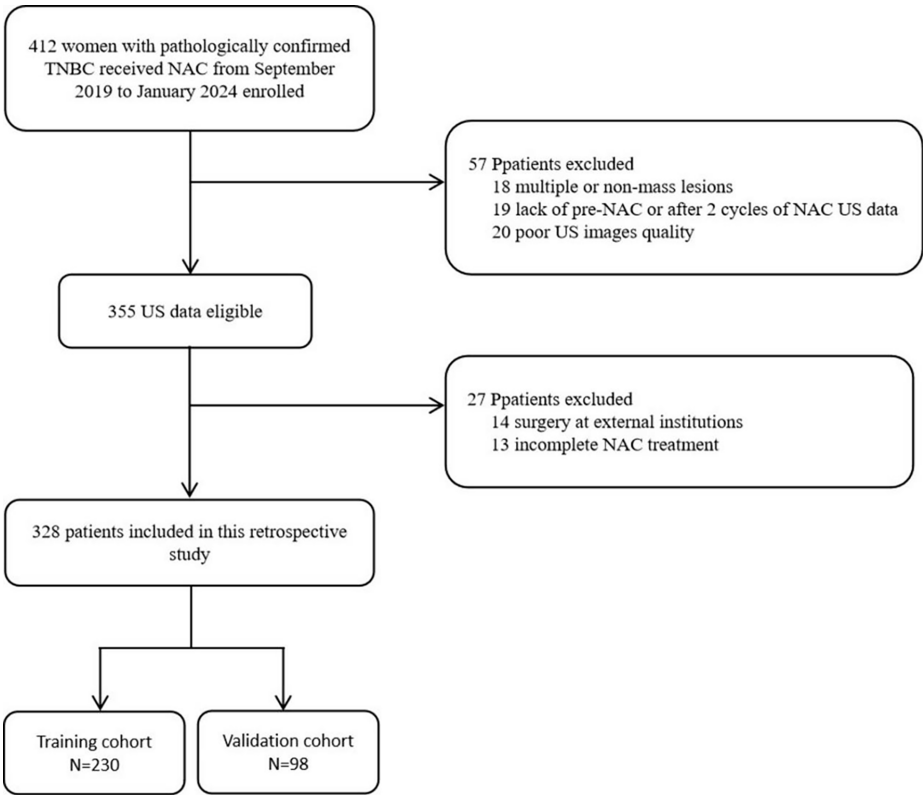
Figure 1. Flowchart showing the study exclusion criteria. TNBC, triple-negative breast cancer; NAC, neoadjuvant chemotherapy; US, ultrasound.

longitudinal views, calcification, posterior echo, blood flow, and axillary lymph node status. Measurements were obtained by two experienced breast sonographers (each with >5 years of work experience) who were blinded to the clinical information.

The tumor volume reduction (TVR) percentage between the pre-NAC and after two cycles of NAC was calculated using the formula:[12]

$$Volume = Length \times Width \times Height \times 0.52 ,$$

$$TVR = (V0 - V2)/V0$$

where V0 is the pre-NAC tumor volume and V2 is the tumor volume after two cycles of NAC.

Clinicopathologic data acquisition and analysis

Clinical and pathological information, including age, menstrual status, and histologic grade, was collected from institutional archives. TNBC was defined by negative expression of the estrogen receptor, progesterone receptor, and HER-2. For HER-2 assessment, immunohistochemistry scores of 0 or 1+ were classified as HER-2 negative, and tumors with immunohistochemical staining of 2+ that lacked HER-2 amplification by fluorescence in situ hybridization were also defined as HER-2 negative.[22]

Chemotherapy and pathologic response evaluation

All included patients received four cycles of epirubicin and cyclophosphamide once every 2 weeks, followed by four additional cycles of either the same regimen or taxane-based treatment. In this study, the US response was evaluated after the first two cycles of epirubicin and cyclophosphamide. Surgical specimens were assessed by pathologists. pCR was defined as the absence of invasive carcinoma in the breast and axillary lymph nodes, with ductal carcinoma in situ permitted (ypT0/is ypN0).

Radiomics signature construction

The radiomics workflow is illustrated in Figures 2a and 2b. Pre-treatment US data were collected for the region of interest (ROI) segmentation and feature extraction for all included patients. An experienced breast sonographer manually defined the ROI at the maximal diameter plane along the tumor contour on the US images using ITK-SNAP Version 3.6.0 (www.itksnap.org). Feature stability was assessed by calculating the intraclass correlation coefficient (ICC), and features with an ICC <0.80 were eliminated. To avoid overfitting in reducing the redundancy and dimensionality process, the least absolute shrinkage and selection operator (LASSO) regression algorithm was used to screen for features associated with pCR prediction. The development of the RS involved the linear combination of the corresponding coefficients from the validation and training cohorts.

Development and validation of the nomogram

Clinical data and US features that could indicate candidate risk factors for pCR were identified using univariate analysis, and those with $P < 0.05$ were subsequently incorporated into multiple logistic regression. Features with $P < 0.05$ were considered statistically significant. The clinical and US risk factors were then used to build a clinico-ultrasonic model.

The early US-based radiomic nomogram was created based on the RS and the clinico-ultrasonic characteristics. Therefore, three preoperative prediction models were fitted in the training cohort: (i) RS model, (ii) clinico-ultrasonic model (clinical factors plus US features), and (iii) early US-based radiomics nomogram (RS plus clinico-ultrasonic model).

Receiver operating characteristic (ROC) curve analysis and the area under the curve (AUC) were used to evaluate the three models' diagnostic performance. Delong's validation was then applied to compare the AUCs between models and ascertain whether there were any notable variations in their diagnostic performance. The concordance index (C-index) was used to evaluate nomogram performance, where a C-index value of 0.5 denoted a random chance and 1.0 denoted an exact differentiation of the outcome. The Hosmer–Lemeshow test was used to evaluate differences between the anticipated and actual data. The calibration curve of the nomogram was plotted for the training and validation groups to assess the consistency of the predicted probabilities of pCR with the actual results. Ultimately, by calculating the net benefit at various threshold probabilities, a decision curve analysis was conducted to evaluate the clinical validity of the radiomics nomogram model.

Statistical analysis

All statistical tests were performed using SPSS software (version 26.0; IBM, Armonk, NY, USA) and R software (version 4.1.2), and a two-tailed $P < 0.05$ was deemed statistically significant. Quantitative variables were compared between the training and validation cohorts using the t-test. Categorical variables were compared using Fisher's exact test or the chi-square test. Continuous variables were presented as mean ± standard deviation. The LASSO logistic regression analysis was performed using the glmnet package. The ROC curve was plotted using the pROC
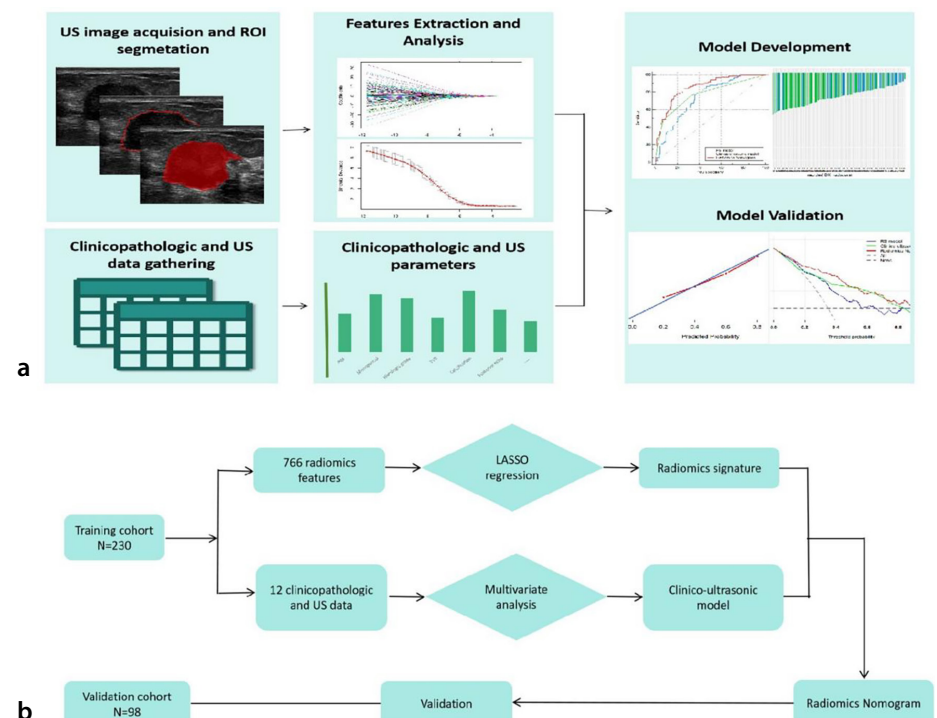
Figure 2. (a) Radiomics workflow and (b) study flowchart. US, ultrasound; ROI, region of interest.

package. The nomogram, calibration curves, and decision curve were created using the rms and rmda software packages. The Hmisc package was used to calculate the C-index.

Results

Patient characteristics and clinico-ultrasonic model

A total of 328 patients meeting the eligibility criteria between September 2019 and January 2024 were included. The overall pCR rate was 34.76% (114 of 328). There was no significant difference in pCR rates between the training and validation cohorts [35.7% (82/230) and 32.7% (32/98), respectively, P = 0.602; Table 1]. Histologic grade and TVR were significantly associated with pCR rate (both $P < 0.05$), and multiple logistic regression analysis revealed that both variables were independent clinical risk predictors for

Table 1. Clinical, histopathological, and US characteristics of the patients in the training and validation cohorts

Characteristics	Training cohort (n = 230)		P	Validation cohort (n = 98)		P
	pCR (n = 148)	non-pCR (n = 82)		pCR (n = 66)	non-pCR (n = 32)	
Age (years, mean ± SD)	49.2 ± 11.8	49.8 ± 9.7	0.692	49.9 ± 9.2	48.4 ± 10.0	0.471
Histologic grade						
I–II	42 (28.4%)	40 (48.8%)	0.002	15 (22.7%)	21 (65.6%)	<0.001
III	106 (71.6%)	42 (51.2%)		51 (77.3%)	11 (34.4%)	
Menopausal status						
Premenopausal	76 (51.4%)	55 (60.4%)	0.008	34 (51.5%)	12 (37.5%)	0.192
Postmenopausal	72 (48.6%)	36 (39.6%)		32 (48.5%)	20 (62.5%)	
US-reported tumor size (mm)						
≤20	18 (12.2%)	14 (17.1%)		3 (4.5%)	3 (9.4%)	
20–50	106 (71.6%)	60 (73.2%)	0.284	52 (78.8%)	24 (75%)	0.646
>50	24 (16.2%)	8 (9.7%)		11 (16.7%)	5 (15.6%)	
Calcification						
Non-calcification	86 (58.1%)	44 (53.7%)	0.514	33 (50%)	21 (65.6%)	0.145
Calcification	62 (41.9%)	38 (46.3%)		33 (50%)	11 (34.4%)	
Posterior echo						
No change	59 (39.9%)	36 (43.9%)		33 (50%)	17 (53.1%)	
Enhancement	24 (16.2%)	17 (20.7%)	0.591	18 (27.3%)	9 (28.1%)	0.964
Shadowing	41 (27.7%)	17 (20.7%)		9 (13.6%)	4 (12.5%)	
Mixed	24 (16.2%)	12 (14.7%)		6 (9.1%)	2 (6.3%)	
Blood flow grade						
0–I	25 (16.9%)	16 (19.5%)	0.619	7 (10.6%)	4 (12.5%)	0.781
II–III	123 (83.1%)	66 (80.5%)		59 (89.4%)	28 (87.5%)	
Resistant index						
≤0.7	53 (35.8%)	39 (47.6%)	0.081	22 (33.3%)	11 (34.4%)	0.918
>0.7	95 (64.2%)	43 (52.4%)		44 (66.7%)	21 (65.6%)	
The number of US-reported abnormal lymph nodes						
None	20 (13.5%)	13 (15.9%)		5 (7.6%)	2 (6.3%)	
≤3	34 (23%)	27 (32.9%)		24 (36.4%)	9 (28.1%)	
3–9	71 (48%)	27 (32.9%)	0.157	29 (43.9%)	16 (50%)	0.835
>9	23 (15.5%)	15 (18.3%)		8 (12.1%)	5 (15.6%)	
Lymph node short/long axis ratio						
≤0.5	82 (55.4%)	48 (58.5%)	0.646	34 (51.5%)	16 (50%)	0.888
>0.5	66 (44.6%)	34 (41.5%)		32 (48.5%)	16 (50%)	
Lymph node type						
Presence of lymphatic gates	85 (57.4%)	58 (70.7%)	0.046	43 (65.2%)	15 (46.9%)	0.084
Disappearance of the lymphatic portal	63 (42.6%)	24 (29.3%)		23 (34.8%)	17 (53.1%)	
TVR						
<80%	138 (93.2%)	43 (52.4%)	<0.001	56 (84.8%)	19 (59.4%)	0.007
≥80%	10 (6.8%)	39 (47.6%)		10 (15.2%)	13 (40.6%)	

SD, standard deviation; pCR, pathologic complete response; US, ultrasound; TVR, tumor volume reduction.

pCR (both $P < 0.05$; Table 2). The clinico-ultrasonic model developed from these two variables performed well in both the training cohort [AUC: 0.773; 95% confidence interval (CI): 0.711–0.835] and the validation cohort (AUC: 0.77; 95% CI: 0.674–0.866). Typical US images from patients with pCR and non-pCR are presented in Figure 3.

Development and validation of the radiomics signature model

From the pre-NAC US images, 766 radiomics features were initially extracted. Using LASSO regression, these were reduced to 12 features with non-zero coefficients. The ICC showed good reproducibility for selected radiomics feature extraction. A heatmap (Figure 4a) illustrates the pairwise correlations between the selected radiomics features. The formula for the final imaging omics score is as follows:

$$\text{Radscore} = -0.606 + \sum_{i=1}^{12} (a_i \times F_i)$$

The specific coefficient (α) and characteristics (F) are shown in Figure 4c. Patients achieving pCR had significantly higher Radscores than those without pCR in both cohorts (all $P < 0.01$, Figure 4b). The RS model exhibited good predictive performance with an AUC of 0.742 (95% CI: 0.678–0.806) in the training cohort and 0.758 (95% CI: 0.646–0.870) in the validation cohort.

Development and performance of the radiomics nomogram

Histologic grade, TVR, and RS were used to construct the early US-based radiomics nomogram (Figure 5), which showed excellent discriminatory power with an AUC of 0.836 (95% CI, 0.807–0.905) in the training cohort and 0.856 (95% CI, 0.749–0.923) in the validation cohort (Figures 6a and 6b). The radiomics nomogram outperformed both the clinico-ultrasonic model (AUC: 0.773, $P < 0.05$) and the RS model (AUC values of 0.742,

$P < 0.05$) in the training cohort (Table 3). The nomogram also performed well in the validation cohort (AUC: 0.856 vs. 0.770, 0.758; $P < 0.05$). The C-index value for predicting pCR

was 0.85 in the training cohort and 0.81 in the validation cohort. Calibration curves for both cohorts showed good alignment with the ideal curve (Figures 6c and 6d), and the
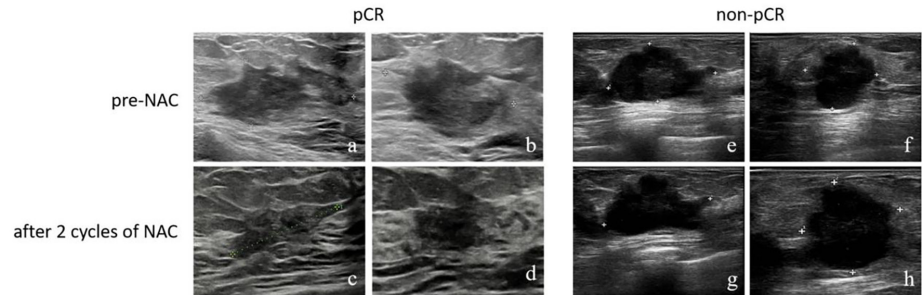

Figure 3. Grey-scale US images. **(a, b)** The three largest tumor dimensions in the transverse and longitudinal images before NAC. **(c, d)** The three largest tumor dimensions in the transverse and longitudinal images after two cycles of NAC. The patient completed neoadjuvant systemic therapy, and surgical pathology confirmed a pCR. **(e, f)** The three largest tumor dimensions in the transverse and longitudinal images before NAC. **(g, h)** The three largest tumor dimensions in the transverse and longitudinal images after two cycles of NAC. The patient completed neoadjuvant systemic therapy, and surgical pathology confirmed a non-pCR. US, ultrasound; NAC, neoadjuvant chemotherapy; pCR, pathologic complete response.
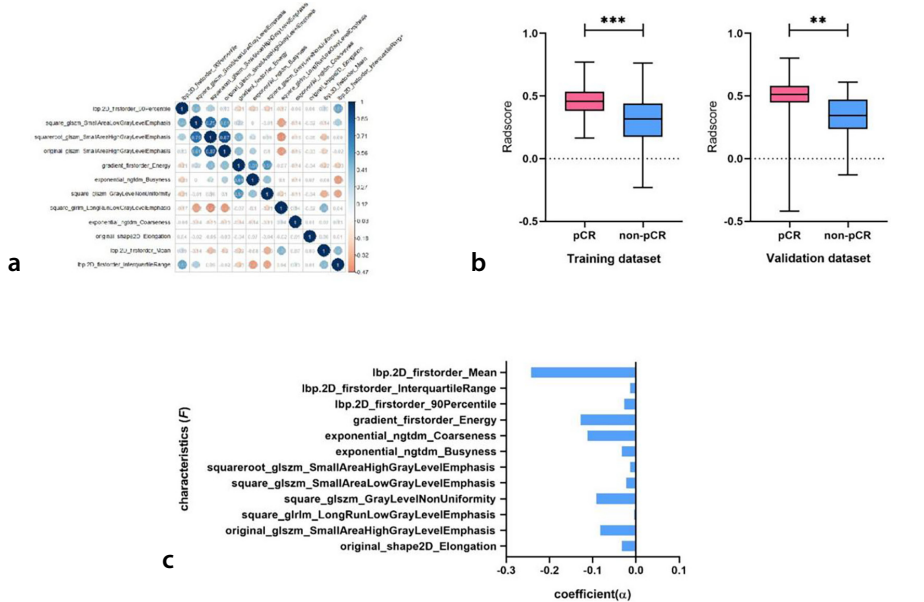

Figure 4. (a) Heatmap of selected radiomics features from the training cohort (GLSZM, grey level size zone matrix; NGTDM, neighboring gray tone difference matrix). **(b)** Comparison of Radscores between the pCR and non-pCR groups in the training and validation cohorts. **(c)** Features selected using LASSO regression. pCR, pathologic complete response; LASSO, least absolute shrinkage and selection operator.

Table 2. Multiple logistic regression analysis of risk factors for pCR						
Characteristics	Training cohort (n = 230)			Validation cohort (n = 98)		
	β	Odds ratio (95% CI)	P	β	Odds ratio (95% CI)	P
Intercept	−0.546			−0.022		
Histologic grade						
I–II		1 (ref)			1 (ref)	
III	−1.050	0.350 (0.183 to 0.668)	0.001	−1.855	0.156 (0.059 to 0.411)	<0.001
TVR						
<80%		1 (ref)			1 (ref)	
≥80%	2.626	13.821 (6.195 to 30.837)	< 0.001	1.318	3.734 (1.270 to 10.977)	0.017
pCR, pathologic complete response; CI, confidence interval; TVR, tumor volume reduction.						

Hosmer–Lemeshow test indicated no significant differences (P = 0.470 and 0.623). Decision curve analysis (Figure 6e) demonstrated that the early US-based radiomics nomogram enhanced the prediction of pCR in breast cancer across a wide range of risk threshold probabilities.

Discussion

In this study, we developed and validated an early US-based radiomics nomogram that integrates clinical data, US features, and RS derived from grayscale US images. The nomogram yielded satisfactory predictions, with an AUC of 0.856 in the training cohort and 0.836 in the validation cohort, outperforming both the clinico-ultrasonic and RS models.

Previous studies have shown that overestimating the extent of residual disease involvement can lead to unnecessary surgical expansion, whereas underestimating the residual cancerous area may result in positive margins and tumor recurrence after NAC in TNBC.[8,10,23,24] However, pathological findings from surgical specimens, considered the gold standard for evaluating NAC effectiveness, are only available after completing chemotherapy. Early prediction of NAC efficacy is therefore essential to allow appropriate therapy adjustments for potentially poor NAC responders. US, MRI, and PET have been investigated in several recent trials to track NAC efficacy, but US, being non-invasive and easily accessible, has an edge over other imaging modalities in predicting early tumor response.[25] A recent study confirmed that combining US features with clinicopathologic factors can accurately predict pCR preoperatively in breast cancer.[15,26] Therefore, we combined clinical prediction factors and US features to develop a clinico-ultrasonic model to predict pCR in patients with TNBC.

Our findings demonstrated a strong correlation between histologic grade and pCR rate in tumors, consistent with recent studies.[27,28] Jung et al.[29] demonstrated that tumors with high histologic grade are associated with improved pCR rates in patients with breast cancer due to their elevated mitotic index, supporting our findings. Ni et al.[30] showed that the changes in maximum tumor diameter after two cycles of NAC, four cycles of NAC, and six cycles of NAC were all independent predictors of pCR (P = 0.017, 0.005 and 0.009), though they did not evaluate TVR across the three largest tumor dimensions, which may be more accurate than predicting NAC efficacy from a single dimension. Adra-

da et al.[12] reported that a reduction of 80% or more in tumor volume after two NAC cycles predicted pCR in patients with TNBC. Gu et al.[31] also stated that the percentage reduction in tumor volume after four cycles was associated with early NAC response in breast cancer patients.

In our study, the optimum cut-off point on the ROC curve was based on the maximal value of the Youden index, and we set the TVR cut-off point to 80%. In the training cohort, the pCR rate was 69.2% (36 of 52) in patients with TVR ≥80% and 25.8% (46 of 178)
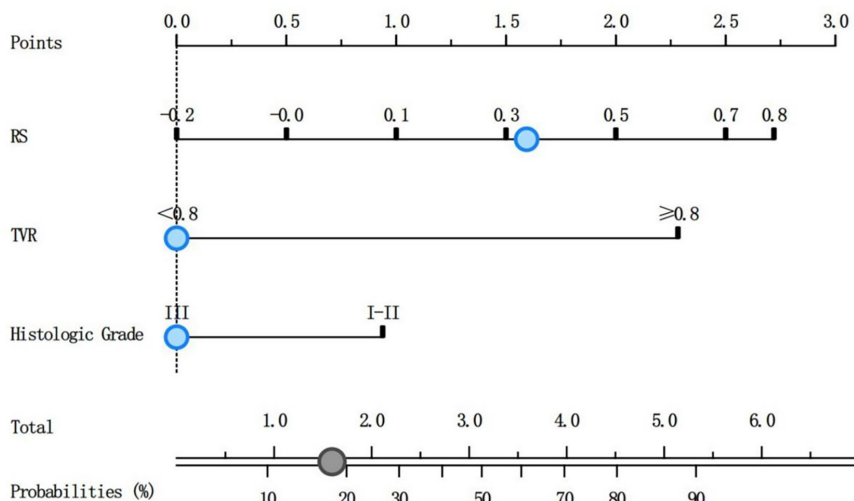

Figure 5. Development of the US-based radiomics nomogram for predicting pCR in TNBC. The nomogram integrates histologic grade, TVR, and RS. US, ultrasound; TNBC, triple-negative breast cancer; TVR, tumor volume reduction; RS, radiomics signature.
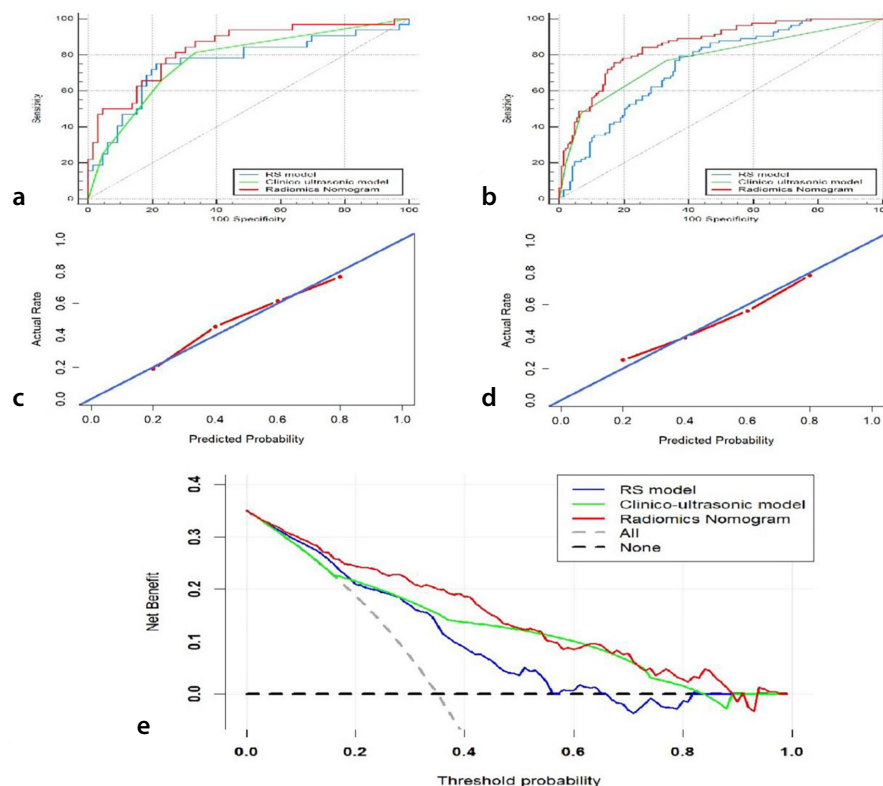

Figure 6. (a, b) ROC comparisons of the clinico-ultrasonic model, RS model, and radiomics nomogram in the training and validation cohorts. **(c, d)** Calibration curves of the radiomics nomogram in the training and validation cohorts. **(e)** Decision curve of the RS model, clinico-ultrasonic model, and radiomics nomogram. ROC, receiver operating characteristic; RS, radiomics signature; pCR, pathologic complete response.

Table 3. Diagnostic performance of the predictive models

Predictive model	Training cohort (n = 230)			Validation cohort (n = 98)		
	Clinico-ultrasonic model	RS model	Radiomics nomogram	Clinico-ultrasonic model	RS model	Radiomics nomogram
AUC (95% CI)	0.773 (95% CI: 0.711–0.835)	0.742 (95% CI: 0.678–0.806)	0.836 (95% CI: 0.807–0.905)	0.770 (95% CI: 0.674–0.866)	0.758 (95% CI: 0.646–0.870)	0.856 (95% CI: 0.749–0.923)
Sensitivity	0.768	0.793	0.756	0.813	0.750	0.667
Specificity	0.669	0.628	0.831	0.667	0.788	0.875
NPV	0.839	0.845	0.860	0.880	0.867	0.917
PPV	0.562	0.542	0.713	0.542	0.632	0.560
C-index	0.85			0.81		

RS, radiomics signature; AUC, area under the curve; CI, confidence interval; PPV, positive predictive value; NPV, negative predictive value; C-index, concordance index.

in patients with TVR <80%. Multiple logistic regression analysis confirmed TVR as an independent risk factor (P < 0.001). Thus, clinical and US features can serve as excellent low-cost predictors in estimating early response in patients with TNBC. No other clinico-ultrasonic factors related to pCR in TNBC were found in this study, possibly due to the low number of patients enrolled.

Radiomics, a computer-aided technology, uses digital medical images to quantify tumor heterogeneity, converting those features into a series of mathematical data.[16,32] Recent studies have shown that radiomics analysis can be used for breast cancer subtype differentiation, therapeutic decision making, and axillary lymph node metastasis prediction.[33-36] Compared with MRI, US images are less expensive, simpler, and easier to obtain for preoperative pCR evaluation, offering substantial potential clinical and financial advantages. In this study, the final RS calculation formula was constructed based on twelve selected radiomics features to predict pCR before surgery in patients with TNBC, revealing excellent predictive performance with an AUC of 0.742 in the training cohort and 0.758 in the validation cohort.

The final twelve radiomics features included one shape-based, four first-order statistical, and seven texture-based features. Among them, the three most valuable were the neighboring gray tone difference matrix (NGTDM) coarseness and first-order mean and energy. First-order mean and energy measured the frequency distribution of the pixel intensity for the zones.[37] In our study, the mammary gland signal intensity correlated with the pCR rate among patients with TNBC. Higher mean and energy may be observed in TNBC non-pCR compared with pCR. The NGTDM coarseness is determined by the variations between voxels in adjacent image planes.[38] Current research indicates biological differences between responsive and

non-responsive tumors, as evidenced by the decreased NGTDM coarseness in pCR compared with non-pCR. In addition, nine other features provided crucial insights into tumor physiology and the microenvironment of pCR, with its multiple tissue components.

Recent advances in radiomics nomograms emphasize the prognostic value of tumor and axillary lymph node status assessment following NAC, thereby informing treatment strategy decisions and avoiding unnecessary surgery.[39] Consequently, to provide an accurate individualized prediction of pCR, we developed a clinically applicable nomogram that integrates clinical data, US features, and RS. Our early US-based radiomics nomogram demonstrated appropriate calibration and excellent discrimination. It outperformed the RS and clinic-ultrasonic models, exhibiting superior predictive performance and net benefit in both the training and validation datasets. Therefore, the nomogram serves as a non-invasive preoperative predictive tool for pCR, helping clinicians identify patients with poor response to NAC and enabling consideration of alternative therapies for chemotherapy-insensitive patients with TNBC. These findings highlight the clinical value of the nomogram.

However, several limitations of this study should be acknowledged. First, this was a retrospective, single-center study, and future studies should involve larger sample sizes and multicenter data. Second, manual ROI segmentation is time-consuming; a fully automatic tool to encourage the clinical application of a nomogram should be explored. Third, elastography and contrast-enhanced US examinations were not included, potentially limiting lesion information and affecting the accuracy of the clinico-ultrasonic model for predicting pCR in TNBC.[40] Fourth, due to the exclusion criteria, patients with multiple cancers or non-mass lesions, and those who lacked pre-NAC or post-two-cy-

cle NAC US data were excluded, potentially resulting in selection bias. Future studies should address these limitations to further refine the current model.

In conclusion, we developed and validated an early US-based radiomics nomogram to predict the likelihood of pCR in patients with TNBC. This tool may assist clinicians in formulating personalized treatment and identifying patients with a high probability of achieving pCR.

Footnotes

Conflict of interest disclosure

The authors declared no conflicts of interest.

References

1. Bray F, Laversanne M, Sung H, et al. Global cancer statistics 2022: GLOBOCAN estimates of incidence and mortality worldwide for 36 cancers in 185 countries. *CA Cancer J Clin*. 2024;74(3)229-263. [Crossref]

2. Jiang YZ, Ma D, Suo C, et al. Genomic and Transcriptomic landscape of triple-negative breast cancers: subtypes and treatment strategies. *Cancer Cell*. 2019;35(3):428-440. [Crossref]

3. Carey L, Winer E, Viale G, Cameron D, Gianni L. Triple-negative breast cancer: disease entity or title of convenience? *Nat Rev Clin Oncol*. 2010;7(12):683-692. [Crossref]

4. Lehmann BD, Bauer JA, Chen X, et al. Identification of human triple-negative breast cancer subtypes and preclinical models for selection of targeted therapies. *J Clin Invest*. 2011;121(7):2750-2767. [Crossref]

5. Foulkes WD, Smith IE, Reis-Filho JS. Triple-negative breast cancer. *N Engl J Med*. 2010;363(20):1938-1948. [Crossref]

6. Verma A, Singh A, Singh MP, et al. EZH2-H3K27me3 mediated KRT14 upregulation promotes TNBC peritoneal metastasis. *Nat Commun*. 2022;13(1):7344. [Crossref]

7. Zagami P, Carey LA. Triple negative breast cancer: pitfalls and progress. *NPJ Breast Cancer*. 2022;8(1):95. [Crossref]

8. Masuda N, Lee SJ, Ohtani S, et al. Adjuvant capecitabine for breast cancer after preoperative chemotherapy. *N Engl J Med*. 2017;376(22):2147-2159. [Crossref]

9. Cortazar P, Zhang L, Untch M, et al. Pathological complete response and long-term clinical benefit in breast cancer: the CTNeoBC pooled analysis. *Lancet*. 2014;384(9938):164-172. Erratum in: *Lancet*. 2019;393(10175):986. [Crossref]

10. Spring L, Greenup R, Niemierko A, et al. Pathologic complete response after neoadjuvant chemotherapy and long-term outcomes among young women with breast cancer. *J Natl Compr Cancer Netw*. 2017;15(10):1216-1223. [Crossref]

11. Pinder SE, Provenzano E, Earl H, Ellis IO. Laboratory handling and histology reporting of breast specimens from patients who have received neoadjuvant chemotherapy. *Histopathology*. 2007;50(4):409-417. [Crossref]

12. Adrada BE, Candelaria R, Moulder S, et al. Early ultrasound evaluation identifies excellent responders to neoadjuvant systemic therapy among patients with triple-negative breast cancer. *Cancer*. 2021;127(16):2880-2887. [Crossref]

13. Rauch GM, Adrada BE, Kuerer HM, van la Parra RF, Leung JW, Yang WT. Multimodality imaging for evaluating response to neoadjuvant chemotherapy in breast cancer. *AJR Am J Roentgenol*. 2017;208:290-299. [Crossref]

14. Fowler AM, Mankoff DA, Joe BN. Imaging neoadjuvant therapy response in breast cancer. *Radiology*. 2017;285(2):358-375. [Crossref]

15. Zhang MQ, Du Y, Zha HL, et al. Construction and validation of a personalized nomogram of ultrasound for pretreatment prediction of breast cancer patients sensitive to neoadjuvant chemotherapy. *Br J Radiol*. 2022;95(1140):20220626. [Crossref]

16. Mayerhoefer ME, Materka A, Langs G, et al. Introduction to radiomics. *J Nucl Med*. 2020;61(4):488-495. [Crossref]

17. Lambin P, Leijenaar RTH, Deist TM, et al. Radiomics: the bridge between medical imaging and personalized medicine. *Nat Rev Clin Oncol*. 2017;14(12):749-762. [Crossref]

18. Jiang M, Li CL, Luo XM, et al. Ultrasound-based deep learning radiomics in the assessment of pathological complete response to neoadjuvant chemotherapy in locally advanced breast cancer. *Eur J Cancer*. 2021;147:95-105. [Crossref]

19. Wibmer A, Hricak H, Gondo T, et al. Haralick texture analysis of prostate MRI: utility for differentiating non-cancerous prostate from prostate cancer and differentiating prostate cancers with different Gleason scores. *Eur Radiol*. 2015;25(10):2840-2850. [Crossref]

20. Du Y, Zha HL, Wang H, et al. Ultrasound-based radiomics nomogram for differentiation of triple-negative breast cancer from fibroadenoma. *Br J Radiol*. 2022;95(1133):20210598. [Crossref]

21. Braman NM, Etesami M, Prasanna P, et al. Intratumoral and peritumoral radiomics for the pretreatment prediction of pathological complete response to neoadjuvant chemotherapy based on breast DCE-MRI. *Breast Cancer Res BCR*. 2017;19(1):57. Erratum in: *Breast Cancer Res*. 2017;19(1):80. [Crossref]

22. Brown M, Tsodikov A, Bauer KR, Parise CA, Caggiano V. The role of human epidermal growth factor receptor 2 in the survival of women with estrogen and progesterone receptor-negative, invasive breast cancer: the California Cancer Registry, 1999-2004. *Cancer*. 2008;112(4):737-747. [Crossref]

23. Ma M, Gan L, Liu Y, et al. Radiomics features based on automatic segmented MRI images: prognostic biomarkers for triple-negative breast cancer treated with neoadjuvant chemotherapy. *Eur J Radiol*. 2022;146:110095. [Crossref]

24. Kuerer HM, Rauch GM, Krishnamurthy S, et al. A clinical feasibility trial for identification of exceptional responders in whom breast cancer surgery can be eliminated following neoadjuvant systemic therapy. *Ann Surg*. 2018;267(5):946-951. [Crossref]

25. Dobruch-Sobczak K, Piotrzkowska-Wróblewska H, Klimonda Z, et al. Multiparametric ultrasound examination for response assessment in breast cancer patients undergoing neoadjuvant therapy. *Sci Rep*. 2021;11(1):2501. [Crossref]

26. Zheng Q, Yan H, He Y, et al. An ultrasound-based nomogram for predicting axillary node pathologic complete response after neoadjuvant chemotherapy in breast cancer: Modeling and external validation. *Cancer*. 2024;130(S8):1513-1523. [Crossref]

27. Liedtke C, Hatzis C, Symmans WF, et al. Genomic grade index is associated with response to chemotherapy in patients with breast cancer. *J Clin Oncol*. 2009;27(19):3185-3191. [Crossref]

28. Hatzis C, Pusztai L, Valero V, et al. A genomic predictor of response and survival following taxane-anthracycline chemotherapy for invasive breast cancer. *JAMA*. 2011;305(18):1873-1881. [Crossref]

29. Jung YY, Hyun CL, Jin MS, et al. Histomorphological factors predicting the response to neoadjuvant chemotherapy in triple-negative breast cancer. *J Breast Cancer*. 2016;19(3):261-267. [Crossref]

30. Ni P, Li Y, Wang Y, et al. Construction of a nomogram prediction model for the pathological complete response after neoadjuvant chemotherapy in breast cancer: a study based on ultrasound and clinicopathological features. *Front Oncol*. 2025;15:1459914. [Crossref]

31. Gu J, Tong T, He C, et al. Deep learning radiomics of ultrasonography can predict response to neoadjuvant chemotherapy in breast cancer at an early stage of treatment: a prospective study. *Eur Radiol*. 2022;32(3):2099-2109. [Crossref]

32. Gillies RJ, Kinahan PE, Hricak H. Radiomics: images are more than pictures, they are data. *Radiology*. 2016;278(2):563-577. [Crossref]

33. Bi WL, Hosny A, Schabath MB, et al. Artificial intelligence in cancer imaging: clinical challenges and applications. *CA Cancer J Clin*. 2019;69(2):127-157. [Crossref]

34. Zheng X, Yao Z, Huang Y, et al. Deep learning radiomics can predict axillary lymph node status in early-stage breast cancer. *Nat Commun*. 2020;11(1):1236. [Crossref]

35. Granzier RWY, Ibrahim A, Primakov SP, et al. MRI-based radiomics analysis for the pretreatment prediction of pathologic complete tumor response to neoadjuvant systemic therapy in breast cancer patients: a multicenter study. *Cancers*. 2021;13(10):2447. [Crossref]

36. Yang M, Liu H, Dai Q, et al. Treatment response prediction using ultrasound-based pre-, post-early, and delta radiomics in neoadjuvant chemotherapy in breast cancer. *Front Oncol*. 2022;12:748008. [Crossref]

37. Nougaret S, Tibermacine H, Tardieu M, Sala E. Radiomics: an introductory guide to what it may foretell. *Curr Oncol Rep*. 2019;21(8):70. [Crossref]

38. Suga M, Nishii R, Miwa K, et al. Differentiation between non-small cell lung cancer and radiation pneumonitis after carbon-ion radiotherapy by 18F-FDG PET/CT texture analysis. *Sci Rep*. 2021;11(1):11509. [Crossref]

39. Gu J, Tong T, Xu D, et al. Deep learning radiomics of ultrasonography for comprehensively predicting tumor and axillary lymph node status after neoadjuvant chemotherapy in breast cancer patients: a multicenter study. *Cancer*. 2023;129(3):356-366. [Crossref]

40. Gu J, Polley EC, Denis M, et al. Early assessment of shear wave elastography parameters foresees the response to neoadjuvant chemotherapy in patients with invasive breast cancer. *Breast Cancer Res*. 2021;23(1):52. [Crossref]